

# Accepted Manuscript

Application of Fe(II)/peroxymonosulfate for improving ultrafiltration membrane performance in surface water treatment: Comparison with coagulation and ozonation

Xiaoxiang Cheng, Heng Liang, An Ding, Xuewu Zhu, Xiaobin Tang, Zhendong Gan, Jiajian Xing, Daoji Wu, Guibai Li



PII: S0043-1354(17)30635-8

DOI: [10.1016/j.watres.2017.07.062](https://doi.org/10.1016/j.watres.2017.07.062)

Reference: WR 13105

To appear in: *Water Research*

Received Date: 16 April 2017

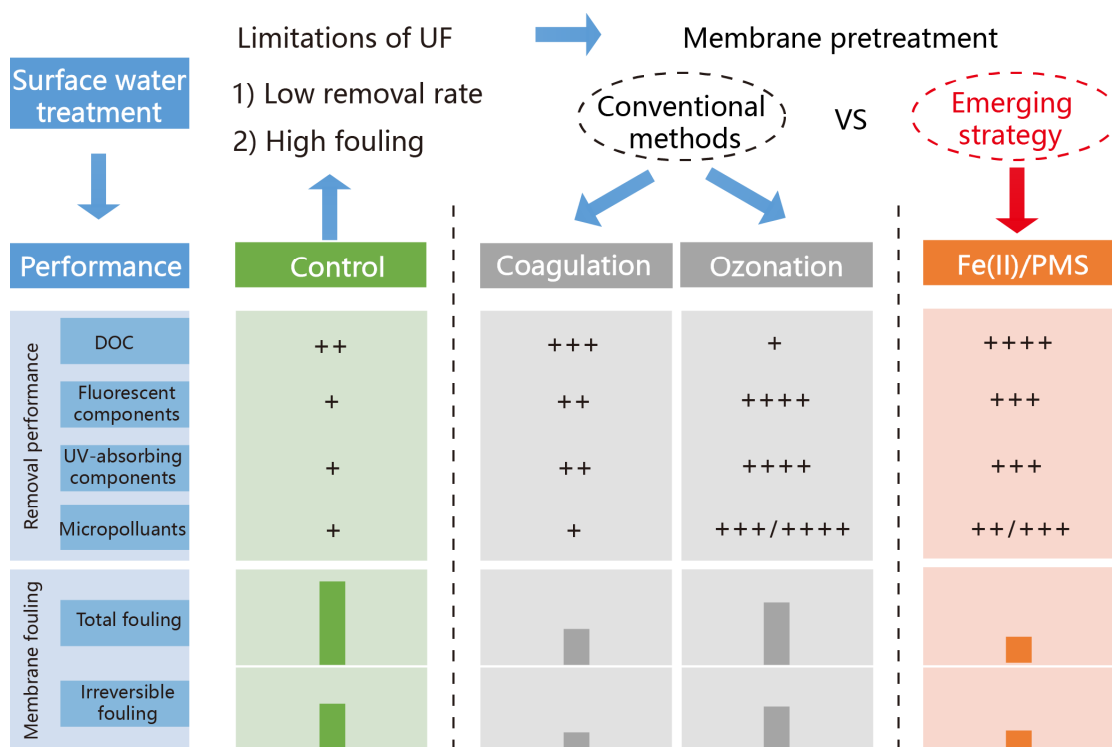
Revised Date: 21 July 2017

Accepted Date: 23 July 2017

Please cite this article as: Cheng, X., Liang, H., Ding, A., Zhu, X., Tang, X., Gan, Z., Xing, J., Wu, D., Li, G., Application of Fe(II)/peroxymonosulfate for improving ultrafiltration membrane performance in surface water treatment: Comparison with coagulation and ozonation, *Water Research* (2017), doi: 10.1016/j.watres.2017.07.062.

This is a PDF file of an unedited manuscript that has been accepted for publication. As a service to our customers we are providing this early version of the manuscript. The manuscript will undergo copyediting, typesetting, and review of the resulting proof before it is published in its final form. Please note that during the production process errors may be discovered which could affect the content, and all legal disclaimers that apply to the journal pertain.

# Graphical Abstract



Revised Manuscript for *Water Research*

Date: 2017-07-21

**Application of Fe(II)/peroxymonosulfate for improving ultrafiltration membrane performance in surface water treatment: Comparison with coagulation and ozonation**

*Xiaoxiang Cheng<sup>a</sup>, Heng Liang<sup>a,\*</sup>, An Ding<sup>a</sup>, Xuewu Zhu<sup>a</sup>, Xiaobin Tang<sup>a</sup>, Zhendong Gan<sup>a</sup>, Jiajian Xing<sup>a</sup>, Daoji Wu<sup>b</sup>, Guibai Li<sup>a</sup>*

<sup>a</sup> *State Key Laboratory of Urban Water Resource and Environment (SKLUWRE), Harbin Institute of Technology, 73 Huanghe Road, Nangang District, Harbin 150090, P.R. China*

<sup>b</sup> *School of Municipal and Environmental Engineering, Shandong Jianzhu University, 1000 Fengming Road, Licheng District, Jinan 250101, P.R. China*

*(E-mail addresses: cxx19890823@163.com (X. Cheng); hitliangheng@163.com (H. Liang); dinganhit@gmail.com (A. Ding); zhuxuewu1314@163.com (X. Zhu); tang5462@163.com (X. Tang); ganzhendong\_hit@163.com (Z. Gan); hitxingjiajian@163.com (J. Xing); wdj@sdjzu.edu.cn (D. Wu); hitsteven@gmail.com (G. Li))*

\*Corresponding author.

Tel.: +86 451 86283001; Fax: +86 451 86283001.

E-mail address: hitliangheng@163.com (Heng Liang).

**ABSTRACT**

Coagulation and ozonation have been widely used as pretreatments for ultrafiltration (UF) membrane in drinking water treatment. While beneficial, coagulation or ozonation alone is unable to both efficiently control membrane fouling and product water quality in many cases. Thus, in this study an emerging alternative of ferrous iron/peroxymonosulfate (Fe(II)/PMS), which can act as both an oxidant and a coagulant was employed prior to UF for treatment of natural surface water, and compared with conventional coagulation and ozonation. The results showed that the Fe(II)/PMS-UF system exhibited the best performance for dissolved organic carbon removal, likely due to the dual functions of coagulation and oxidation in the single process. The fluorescent and UV-absorbing organic components were more susceptible to ozonation than Fe(II)/PMS treatment. Fe(II)/PMS and ozonation pretreatments significantly increased the removal efficiency of atrazine, *p*-chloronitrobenzene and sulfamethazine by 12–76% and 50–94%, respectively, whereas coagulation exerted a minor influence. The Fe(II)/PMS pretreatment also showed the best performance for the reduction of both reversible and irreversible membrane fouling, and the performance was hardly affected by membrane pore size and surface hydrophobicity. In addition, the characterization of hydraulic irreversible organic foulants confirmed its effectiveness. These results demonstrate the potential advantages of applying Fe(II)/PMS as a pretreatment for UF to simultaneously control membrane fouling and improve the permeate quality.

**Key words:** Ferrous iron/peroxymonosulfate (Fe(II)/PMS), coagulation, ozonation,

23 ultrafiltration (UF) membrane, membrane fouling

## 1. Introduction

Ultrafiltration (UF) membrane has been increasingly used in water and wastewater treatment, but some drawbacks are still limitations to its widespread application, such as membrane fouling and insufficient removal of relatively smaller organic foulants (Lee et al., 2004). Many strategies have been proposed to improve the performance of UF membrane, among which feed water pretreatments have drawn much attention in recent years (Gao et al., 2011; Huang et al., 2009). The widely used pretreatment methods include coagulation (Tian et al., 2008), adsorption (Stoquart et al., 2012), oxidation (Van Geluwe et al., 2011), filtration (Yu and Graham, 2015), etc. Although most of these methods were reported to be effective, some problems still occurred in many cases. Yu et al. (2016a) reported that pre-coagulation could only remove a proportion of biopolymers in the feed water, and the remainder together with bacteria and residual flocs invariably accumulated on the membrane. To solve this problem, an additional treatment of pulsed ultraviolet (UV)-irradiation was employed to more effectively control membrane fouling. The combination of different methods was generally shown to be more effective than a single treatment, such as coagulation-ozonation (the addition of low-dose ozone was effective for fully mitigating membrane fouling) (Yu et al., 2016b), and coagulation-powdered activated carbon adsorption combined with in situ chlorination led to further alleviation of membrane fouling (Wang et al., 2016).

Recently, hydroxyl radical ( $\cdot\text{OH}$ )-based advanced oxidation processes (HR-AOPs) have been proposed to integrate with membrane filtration, such as UV/H<sub>2</sub>O<sub>2</sub> (Zhang et

al., 2015), and ozonation/H<sub>2</sub>O<sub>2</sub> (Zouboulis et al., 2014). Compared with HR-AOPs, sulfate radicals (SO<sub>4</sub><sup>•-</sup>)-based advanced oxidation processes (SR-AOPs) are gaining popularity for contaminant degradation in aqueous solutions. SO<sub>4</sub><sup>•-</sup> has been known as a strong oxidant for its high standard redox potential ( $E_0 = 2.6$  V vs NHE), which is comparable to that of <sup>•</sup>OH ( $E_0 = 2.73$  V vs NHE) (Luo et al., 2015). SO<sub>4</sub><sup>•-</sup> can be generated from activation of persulfate (PS) or peroxymonosulfate (PMS) by the methods of heat, ultrasonic, UV, and transition metal ions (Antoniou et al., 2010; Rastogi et al., 2009b). It is generally accepted that SO<sub>4</sub><sup>•-</sup> has a longer half-life and reacts more selectively with organic compounds than <sup>•</sup>OH due to one electron transfer mechanism (Ji et al., 2014; Rastogi et al., 2009b). Therefore, SR-AOPs are normally considered to be less influenced by water matrix composition and effective for the degradation of recalcitrant organic compounds. In previous research, SR-AOPs have been studied in the degradation of organic contaminants, such as atrazine (Anipsitakis and Dionysiou, 2003), 2,4-dichlorophenol (Anipsitakis and Dionysiou, 2004), etc. Whereas, to the best of our knowledge, very limited work on their application for membrane pretreatment has been done. Considering the strong oxidation characteristics of SO<sub>4</sub><sup>•-</sup>, SR-AOPs may have the potential for improving membrane performance by decreasing the concentration of membrane foulants as well as micropollutants. Hence, it is of particular interest to integrate SR-AOPs pretreatment with UF membrane to simultaneously control membrane fouling and product water quality.

In this study, PMS was chosen as an oxidant alternative due to its universal

activation nature over PS and  $\text{H}_2\text{O}_2$  (Rastogi et al., 2009b). Compared with heat, ultrasonic or UV, transition metal based activation is the most promising method for field application because it is more convenient to apply and adds relatively lower cost. Thus, ferrous iron ( $\text{Fe(II)}$ ) was selected as an ideal activator owing to its higher activity and environmentally friendly nature (Zou et al., 2013). To avoid iron speciation and precipitation, previous studies on the  $\text{Fe(II)}$ -activated PMS process mainly conducted at pH around 3.0 (Ji et al., 2015), or at neutral pH conditions in the presence of chelating agents (Rastogi et al., 2009a). In our recent study (Cheng et al., 2017),  $\text{Fe(II)}$ /PMS was employed as a membrane pretreatment to treat surrogate organic compounds in neutral water. It was shown that  $\text{Fe(II)}$ /PMS was very effective for both membrane fouling control and trace organic removal, which was mainly due to the dual functions of coagulation and oxidation. However, it should be noted that there might be some discrepancies between surrogate organic compounds and real water samples. Therefore, it is necessary to evaluate the effectiveness of  $\text{Fe(II)}$ /PMS as membrane pretreatment for natural waters, especially when its practical value is advocated.

To better understand the emerging alternative, two widely applied pretreatment strategies for UF membrane, including coagulation and ozonation were also employed for comparison with  $\text{Fe(II)}$ /PMS. The effects of these methods on the removal performance of organic pollutants and membrane fouling control were investigated in the treatment of natural surface water. Four types of UF membranes with different pore sizes and materials were employed to verify the feasibility of  $\text{Fe(II)}$ /PMS



pretreatment. Moreover, fluorescence excitation-emission matrix (EEM) and size exclusion chromatography (SEC) were utilized to characterize membrane fouling. The experimental results indicated that Fe(II)/PMS pretreatment showed a major improvement in membrane performance.

## 2. Materials and methods

### 2.1 Raw water

In this study, a natural surface water collected from Songhua River (Northeast China) was employed as raw water. Prior to the experiment, the collected water sample was stored in a pre-sedimentation tank placed in the laboratory, and the water temperature was kept constant at  $20\pm1^{\circ}\text{C}$ . The water qualities are listed as follows: turbidity: 1.16–2.58 NTU, dissolved organic carbon (DOC) concentration: 7.62–8.41 mg/L, ultraviolet absorbance ( $\text{UV}_{254}$ ):  $0.093\text{--}0.110\text{ cm}^{-1}$ , dissolved oxygen concentration: 6.0–8.0 mg/L, and pH: 6.8–7.3.

### 2.2 Experimental setup

#### 2.2.1 Pretreatments

Fe(II)-activated PMS, Fe(III) coagulation and ozonation were adopted as pretreatment alternatives for UF membranes. A commercially available potassium peroxymonosulfate triple salt ( $2\text{KHSO}_5\cdot\text{KHSO}_4\cdot\text{K}_2\text{SO}_4$ ) was supplied by Aladdin Chemicals (Shanghai, China). Ferrous sulfate ( $\text{FeSO}_4$ ) and ferric chloride ( $\text{FeCl}_3$ ) were of guaranteed reagent grade quality and purchased from Bench Chemicals (Tianjin, China). The stock solutions of  $\text{FeSO}_4$ ,  $\text{FeCl}_3$  and PMS were all freshly prepared by dissolving weighed amounts of solids in ultrapure water.  $\text{FeSO}_4$  and

FeCl<sub>3</sub> were analyzed by inductively coupled plasma optical emission spectrometry, and PMS by iodometric method (Ball et al., 1967). The Fe(II)/PMS pretreatment was conducted in triangular flasks, which was initiated by adding desirable doses of PMS into the samples containing Fe(II) at certain concentrations. In the coagulation experiment, certain doses of Fe(III) were added into water samples to start the reaction. The pretreatments were performed with rapid mixing for 1 min at 200 r/min, followed by slow mixing for 20 min at 50 r/min. Ozone gas was generated by passing high purity oxygen gas through an ozone generator (LAB2B, Ozonia, England). The detail of pre-ozonation experiment was described in our previous study (Cheng et al., 2016). The same molar dose (100 µmol/L, if not otherwise specified) of Fe(II)/PMS (with molar ratio of 1:1), Fe(III) and ozone was employed for feed water pretreatment, and the pretreated water samples were subsequently used for membrane filtration.

### 2.2.2 Membrane filtration

Four types of commercially available flat-sheet UF membranes with different pore sizes and surface hydrophobicities were employed in the filtration experiment, including a polyethersulfone (PES) membrane (Microdyn-Nadir, Germany) with molecular weight cutoff (MWCO) of 150 kDa, and ceramic membranes (TAMI, France) with MWCO of 150, 50 and 5 kDa (denoted PES150, CM150, CM50 and CM5, respectively). It should be noted that PES membrane shows relatively lower antioxidant ability than ceramic membrane. PES150 with a contact angle of 65.7° was much more hydrophobic than CM150 which had a contact angle of 28.3°. The contact angle was measured by the standard sessile drop method using a contact angle

measurement system (JYSP-360, Beijing United Test Co., Ltd., China), and membrane surface roughness was analyzed by atomic force microscopy (Bioscope, Veeco, USA). The characteristics of employed membranes are shown in Table 1. If not otherwise specified, the commonly used membrane in this study was CM50.

Fig. 1 shows the experiment setup of UF, Fe(II)/PMS-UF (FPUF), coagulation-UF (CUF) and ozonation-UF (OUF). Raw water, as well as water samples pretreated by Fe(II)/PMS, coagulation and ozonation were utilized for membrane filtration. The filtration experiment was performed in filtration cells with dead-end mode. The filtration cell for ceramic membrane was made of plexiglass with an effective volume of 120 mL, and PES membrane filtration was performed in a filtration cell (Amicon 8400, Millipore, USA) with an effective volume of 400 mL. A nitrogen gas bottle connected to the filtration cell was used to maintain the constant transmembrane pressure (TMP) of 100 kPa. The UF membranes were placed at the bottom of the filtration cell during the experiment and each filtration test was run with three cycles.

**Table 1**

**Fig. 1**

### **2.3 Fouling resistance analysis**

The resistance-in-series model (Lin et al., 2009) was used to evaluate the fouling resistance. The total resistance ( $R_t$ ) consists of intrinsic membrane resistance ( $R_m$ ), hydraulic reversible fouling resistance ( $R_r$ ) and hydraulic irreversible fouling resistance ( $R_{ir}$ ). Specifically,  $R_m$  was calculated through the ultrapure water flux of

virgin membrane ( $J_0$ ) (Eq. (1)).  $R_t$  was measured according to the final permeate flux ( $J_t$ ) of fouled membrane (Eq. (2)).  $R_r$  and  $R_{ir}$  were calculated by the ultrapure water flux of membrane after hydraulic backwash ( $J_2$ ) (Eqs. (3) and (4)). In this study, hydraulic backwash was conducted with ultrapure water by applying a relatively higher pressure on the permeate side, forcing ultrapure water back through the membrane to the feed side. To avoid destroying the membrane (especially PES membrane) during backwash, the pressure and backwash time were controlled at 150 kPa and 2 min, respectively. The integrity of the membrane after backwash was assured by measuring the pure water flux of membrane.

$$R_m = TMP/(\mu J_0) \quad (1)$$

$$R_t = TMP/(\mu J_t) \quad (2)$$

$$R_r = TMP/(\mu J_1) - TMP/(\mu J_2) \quad (3)$$

$$R_{ir} = R_t - R_m - R_r = TMP/(\mu J_2) - TMP/(\mu J_0) \quad (4)$$

where,  $R$  is the filtration resistance ( $\text{m}^{-1}$ ),  $TMP$  is the transmembrane pressure (Pa),  $\mu$  is the dynamic viscosity (Pa·s),  $J$  is the permeate flux ( $\text{m}^3/\text{m}^2\cdot\text{s}$ ).

## 2.4 Analytical methods

### 2.4.1 Fluorescence excitation-emission matrix (EEM) analysis

EEM was employed to characterize the fluorescent components in the water and the organic foulants deposited in membrane pores. The EEM spectra was generated using a fluorescence spectrophotometer (F7000, Hitachi, Japan) with excitation (Ex) wavelengths of 200–450 nm and emission (Em) wavelengths of 250–550 nm. The EEM spectrum of ultrapure water was subtracted from each sample EEM to remove

most of the Raman scatter peaks. All EEM data were Raman calibrated and the fluorescence intensities were reported in Raman units (R.U.,  $\text{nm}^{-1}$ ) (Murphy et al., 2010). In addition, a parallel factor analysis (PARAFAC) was used to identify the fluorescent components in the Songhua River (Shao et al., 2014).

#### 2.4.2 Size exclusion chromatography (SEC) analysis

To determine the apparent molecular weight (MW) distributions of natural organic matter (NOM) in the raw and treated water samples, a size exclusion chromatography coupled with a UV detector (SEC-UV) was used in this study. The measurement was performed by using a high-performance liquid chromatograph (HPLC, Agilent 1200) and a TSK-gel G4000PW<sub>XL</sub> silica gel column (7.8×300 mm, 10  $\mu\text{m}$ ) (TOSOH, Japan). The mobile phase consisted of 0.1 mol/L NaCl, 0.002 mol/L  $\text{K}_2\text{HPO}_4$  and 0.002 mol/L  $\text{KH}_2\text{PO}_4$  (phosphate buffer solution, pH=6.85). The flow rate was set as 0.3 mL/min and the injection volume of water sample was controlled at 100  $\mu\text{L}$ . The calibration was carried out by sodium polystyrene sulfonates standards with MW of 3, 7, 15, 80 and 130 kDa, respectively (Fig. S1).

#### 2.4.3 Analysis of micropollutants

Atrazine (ATZ), *p*-chloronitrobenzene (*p*-CNB) and sulfamethazine (SMT) were employed to evaluate the removal performance of micropollutants. ATZ and SMT were purchased from Sigma-Aldrich (USA), and *p*-CNB was supplied by Aladdin Chemicals (Shanghai, China). During the experiment, ATZ, *p*-CNB and SMT were individually spiked into the feed water with the same molar concentration of 1  $\mu\text{mol/L}$ , corresponding to the concentrations of 216, 158 and 278  $\mu\text{g/L}$ , respectively. The

micropollutants were measured by HPLC coupled with a UV detector. Chromatographic separations were performed using a Spherisorb S5 ODS2 column (4.6×250 mm, 5 µm) (Waters, USA) with an eluent flow rate of 1.0 mL/min and a column temperature of 30°C. The concentration of ATZ was quantified at a wavelength of 225 nm using an eluent of ultrapure water/methanol (30:70, v/v). The concentration of *p*-CNB was measured using an eluent of ultrapure water/methanol (20:80, v/v) at a wavelength of 275 nm. SMT was analyzed at a wavelength of 270 nm using an eluent of ultrapure water/methanol (60:40, v/v).

#### 2.4.4 Extraction of hydraulic irreversible foulants

At the end of the experiment, hydraulic irreversible organic foulants were extracted from the membranes (after hydraulic backwash) using 0.01 mol/L NaOH, and the membranes were soaked in the alkaline solution for 24 h at 20°C. The pH of the chemical solution was then adjusted to neutral using HCl solution. The extracted organic foulants were saved at 4°C for further analysis.

#### 2.4.5 Other analytical methods

DOC was measured using a total organic carbon analyzer (multi N/C 2100, Jena, Germany). UV<sub>254</sub> was determined by a UV/vis spectrophotometer (T6, Puxi, China) at the wavelength of 254 nm. Prior to DOC and UV<sub>254</sub> measurements, the samples were pre-filtered by 0.45 µm cellulose ester membranes. The classic fouling models, namely, complete blocking, standard blocking, intermediate blocking and cake filtration (Qu et al., 2014) were used to better understand membrane fouling mechanism. Moreover, an analysis of variance (ANOVA) at the significance level of *p*

< 0.05 was applied by the Microsoft Excel software (Microsoft, USA) to statistically analyze and compare the experimental data. The null hypothesis was that there was no difference between different systems. If  $p < 0.05$ , the null hypothesis was rejected, meaning that the difference was significant. Conversely, the null hypothesis was accepted when  $p > 0.05$ , and the difference was not significant.

### 3. Results and discussion

#### 3.1 Removal of organic pollutants

##### 3.1.1 DOC and UV<sub>254</sub>

Fig.2(a) shows the removal efficiencies of DOC and UV<sub>254</sub>. The average DOC concentrations decreased from 8.1 to 7.3, 5.4, 6.2 and 7.4 mg/L in the systems of UF, FPUF, CUF and OUF, respectively. In addition, all the  $p$  values were below 0.05, suggesting that the difference between the feed and UF permeate of each system was significant. This result also indicated that Fe(II)/PMS pretreatment exhibited better performance in DOC removal than coagulation with the same molar dose of Fe(III). Previous study (Anipsitakis and Dionysiou, 2004) reported that activation of PMS by Fe(II) simultaneously led to the generation of Fe(III) and  $\text{SO}_4^{\bullet-}$ . In neutral aqueous environment, ferric oxyhydroxides were subsequently formed through hydrolysis, and the generated  $\text{SO}_4^{\bullet-}$  promoted the formation of other active species, particularly  $\cdot\text{OH}$  (Cheng et al., 2017). Thus, the *in-situ* formed Fe(III) worked as a coagulant (Guan et al., 2009), and the higher DOC removal rate of FPUF was most likely due to the improvement of coagulation efficiency by  $\text{SO}_4^{\bullet-}$  and  $\cdot\text{OH}$  oxidation (Xie et al., 2016). To be specific, oxidation can change the zeta potential of particles by destroying the

organic coating on their surfaces, which was a main reason for improving coagulation. Moreover, mineralization of some low MW organic matter by  $\text{SO}_4^{\bullet-}$  and  $\cdot\text{OH}$  oxidation also contributed to the reduction of DOC. Compared with single UF, pre-ozonation even slightly increased the permeate DOC concentration of UF. This result was consistent with our previous study (Cheng et al., 2016) that pre-ozonation increased the permeate DOC by converting high-MW organic molecules into small and hydrophilic fragments, which were more likely to pass through membrane pores.

The removal performance of  $\text{UV}_{254}$  was to some extent different from that of DOC. After treatments by UF, FPUF, CUF and OUF, the  $\text{UV}_{254}$  values significantly decreased from 0.102 to 0.077, 0.049, 0.068 and 0.038  $\text{cm}^{-1}$  ( $p < 0.05$ ), corresponding to the removal rates of 25%, 52%, 33% and 63%, respectively. It seemed that OUF showed the best performance in  $\text{UV}_{254}$  removal, which was caused by the strong oxidizing property of ozone.  $\text{UV}_{254}$  mainly represents the organic pollutants containing unsaturated bonds or aromatic chromophores (primarily humics) (Leenheer and Croué, 2003), which was more susceptible to oxidizing agents. Thus, the removal effect of FPUF was also better than CUF. In comparison with the widely used pretreatment methods of coagulation and ozonation, Fe(II)/PMS was an effective method to improve the performance of both DOC and  $\text{UV}_{254}$  removal for UF membranes.

## Fig. 2

### 3.1.2 Fluorescent components

Fluorescent organic matter, which is a crucial issue in UF membrane fouling, can



be sensitively and rapidly detected by EEM. To analyze the fluorescent components in the Songhua River water, PARAFAC analysis was utilized in our previous study (Shao et al., 2014), and three statistically significant components were identified as C1 (Ex/Em = 240(310)/400-450 nm, microbial humic-like substances), C2 (Ex/Em = 270(360)/470 nm, terrestrially derived humic-like substances), and C3 (Ex/Em = 225(280)/340 nm, protein-like substances). The fluorescence EEM spectra of each sample are shown in Fig. S2, and the maximum fluorescence intensity ( $F_{max}$ ) of each component in the feed and permeate are illustrated in Fig.2(b). The  $F_{max}$  for C1, C2 and C3 of the feed water were 0.71, 0.48 and 0.38 R.U., respectively. For all the fluorescent components, the  $p$  values between the feed and UF permeate were above 0.05, suggesting that the difference between the fluorescence intensity of feed and UF permeate was not significant. The results indicated that single UF filtration exerted a minor effect on the removal of fluorescent components (the average removal rate was approximately 10%). The integration of Fe(II)/PMS and coagulation pretreatments with UF significantly reduced the  $F_{max}$  of C1 and C2 ( $p < 0.05$ ), and pre-ozonation simultaneously reduced the  $F_{max}$  of C1, C2 and C3 ( $p < 0.05$ ). At the same molar dose, the removal performance of  $F_{max}$  followed the order of ozonation > Fe(II)/PMS > coagulation, suggesting that pre-oxidation exhibited better  $F_{max}$  removal performance than pre-coagulation, mainly due to the significant change in the fluorescent characteristic of NOM induced by oxidation.

### 3.1.3 SEC-UV chromatograms

The MW distributions of NOM in the feed and permeate were determined by

SEC-UV (Fig.2(c)). According to the MW calibration of SEC-UV (Fig. S1), the main UV-absorbing components in the feed distributed in the range of 1-10 kDa with a peak at approximately 7 kDa, which were mainly composed of humic substances (1-20 kDa), whereas biopolymers (> 20,000 Da), building blocks (300-500 Da) and low MW substances (<350 Da) (Huber et al., 2011) were not detected due to the limitation of the UV detector. After different treatments, the peak of humic substances for the feed was significantly reduced. The overall UV response in the permeate showed the regularity of UF > CUF > FPUF > OUF, indicating that ozonation was more effective for removing UV-absorbing components over a wide MW range than Fe(II)/PMS and coagulation. The similar result has been reported that UV-absorbing compounds were more susceptible to the oxidation treatment by UV/H<sub>2</sub>O<sub>2</sub> than coagulation (Zhang et al., 2015). These results were also consistent with the UV<sub>254</sub> removal in Fig. 2(a).

#### 3.1.4 Micropollutants

#### Fig. 3

The removal efficiencies of micropollutants in different systems are shown in Fig. 3. In the experiment of micropollutants removal, the employed doses of Fe(II)/PMS, Fe(III) and ozone were 50 µmol/L, respectively. As one of the most widely used herbicides, ATZ has been classified as a possible carcinogen and endocrine disrupting chemical, which is a threat to aquatic environment (Ji et al., 2015). As shown in Fig. 3, the UF system showed a limited removal efficiency for ATZ (4.9%). Pretreatments by Fe(II)/PMS and ozonation significantly increased the ATZ removal rate (40% and 71%, respectively,  $p < 0.05$ ), whereas coagulation showed a minor influence (5.0%,  $p >$

0.05). Since the MW of ATZ molecule was much smaller than the membrane pore size, ATZ was difficult to be removed through size exclusion, which is recognized as a core mechanism of UF membrane. Previous studies (Acero et al., 2012) also reported that pre-coagulation preferentially removed high MW components and did not lead to an appreciable reduction of ATZ and other emerging contaminants. In natural waters, iron speciation and precipitation would slow the transformation from Fe(III) to Fe(II), thus decreasing the oxidation effectiveness of Fe(II)/PMS process. In spite of this, Fe(II)/PMS still exhibited certain removal effect for ATZ due to the high reaction constant between  $\text{SO}_4^{\bullet-}$  and ATZ ( $k = 3.0 \times 10^9 \text{ M}^{-1}\text{s}^{-1}$ ) (Lutze et al., 2015). Ozone is known to decompose in aqueous solutions, yielding secondary oxidants such as  $\cdot\text{OH}$  or other radicals (Staehelin and Hoigne, 1985). The oxidation of ATZ by ozone may thus proceed either through direct ozonation or  $\cdot\text{OH}$  attack to the ATZ molecule. Therefore, pre-ozonation showed the best performance for ATZ removal. Both the reactions of  $\text{SO}_4^{\bullet-}$  and  $\cdot\text{OH}$  with ATZ led to dealkylation and correspondingly produced intermediate products, such as desethyl-atrazine and desisopropyl-atrazine (Lutze et al., 2015).

*p*-CNB has been widely used as a synthetic intermediate for the production of various industrial chemicals. It is demonstrated that *p*-CNB has the potential of genotoxicity and carcinogenic, which is not easily biodegraded in water (Wang et al., 2015). Fig. 3 shows that single UF filtration exhibited a poor removal efficiency for *p*-CNB (7.1%). Fe(II)/PMS pretreatment slightly increased the removal efficiency (19%,  $p < 0.05$ ), whereas pre-ozonation significantly improved *p*-CNB removal (57%,

$p < 0.05$ ). The relatively lower improvement of Fe(II)/PMS was likely due to the low reaction constant between  $\text{SO}_4^{\bullet-}$  and nitrobenzene compounds ( $k \leq 10^6 \text{ M}^{-1}\text{s}^{-1}$ ) (Neta et al., 1977). Similar with ATZ, coagulation did not increase the removal effect of *p*-CNB (7.7%,  $p > 0.05$ ) (Fig. 3). In addition, both Fe(II)/PMS and ozonation exhibited relatively lower removal efficiency of *p*-CNB compared with ATZ.

SMT is an antibiotic pharmaceutical product, which has been widely used in human and veterinary medicine and is detected in aquatic environment (Barhoumi et al., 2016). Similar with ATZ and *p*-CNB, both UF and CUF showed poor removal efficiencies for SMT (6.1–6.5%,  $p > 0.05$ ) (Fig. 3). The integration of UF with Fe(II)/PMS dramatically increased the removal efficiency (82%,  $p < 0.05$ ) (Fig. 3), indicating the favorable oxidation behavior of Fe(II)/PMS process. Pre-ozonation showed excellent removal performance for SMT, and it could be completely removed in the OUF system (Fig. 3). The above results indicated that Fe(II)/PMS and ozonation pretreatments could improve the ability of UF membrane to remove micropollutants, whereas coagulation exerted a minor influence.

## 3.2 Membrane fouling control

### 3.2.1 Comparison of pretreatment methods

The flux variations and fouling resistances in the systems of UF, FPUF, CUF and OUF with CM 50 are illustrated in Fig. 4. As seen in Fig. 4(a), the raw water without any pretreatment caused the most severe flux decline with reductions of approximately 37%, 40% and 42% during the first, second and third filtration cycle, respectively. Pre-ozonation significantly improved the flux over all filtration cycles

and the terminal specific flux ( $J_t/J_0$ ) increased from 0.58 to 0.63. Pre-coagulation further promoted the  $J_t/J_0$  to 0.75, and all the three cycles exhibited the same trends. Although both coagulation and ozonation contributed to flux improvement, the mechanisms were considered to be significantly different. Ozonation could completely mineralize some low MW organic molecules and/or partially decompose large molecules into hydrophilic and small substances, inducing less accumulation of organic matter on the membrane surface (Van Geluwe et al., 2011); whereas coagulation decreased the organic loadings of membrane by removing organic matter through binding with insoluble flocs, followed by precipitation. For the FPUF system, the flux curve was only slightly higher than that of CUF in the first cycle, and the flux difference became more significant in the last two cycles (with  $J_t/J_0$  of 0.83). The results indicated that Fe(II)/PMS pretreatment exhibited the best performance in flux improvement for UF membrane.

#### Fig. 4

Fig. 4(b) shows that the values of  $R_t$  and  $R_r$  for single UF were the highest, and the value of  $R_t$  and the proportion of  $R_{ir}$  were gradually increased with the increase of filtration cycle, indicating that raw water caused the most serious membrane fouling. In general, pretreatments prior to UF significantly reduced the total membrane fouling with the reduction rate of 25–69%. Pre-ozonation mainly reduced the values of  $R_t$  and  $R_r$ , whereas the variation of  $R_{ir}$  was not obvious, likely due to the generation of some low MW substances, showing a higher potential to block membrane pores and consequently increased irreversible fouling to some extent (Zhang et al., 2015). By

contrast, both  $R_r$  and  $R_{ir}$  were obviously decreased in the CUF system. Compared with coagulation, Fe(II)/PMS pretreatment further decreased  $R_t$  and  $R_r$ , and its excellent performance may be caused by the following reasons: (1) the coagulation efficiency was enhanced by  $\text{SO}_4^{\bullet-}$  and  $\cdot\text{OH}$  oxidation (Xie et al., 2016); (2) compared with coagulation alone, some low MW organic molecules were mineralized by oxidation; and (3) the addition of oxidation increased the proportion of hydrophilic substances, showing a lower propensity for adsorption on membrane surface (Cheng et al., 2016).

The regression results using fouling models (Table 2) indicated that membrane fouling by the raw water was governed by multiple mechanisms, among which standard blocking ( $R^2 = 0.998$ ) and cake filtration ( $R^2 = 0.970$ ) dominated the fouling formation. This was likely attributed to the diversity of MW distributions for organic matter. To be specific, the low MW organics may adhere inside membrane pores causing standard blocking, whereas the high MW components may be retained on the surface of membrane to form a cake layer (Qu et al., 2014). Although the fouling conditions differed from each other, the regression results of each system changed little (Table 2). In short, pretreatments prior to UF membrane attributed to flux improvement and fouling mitigation, among which Fe(II)/PMS process showed the best performance for the reduction of both reversible and irreversible membrane fouling.

**Table 2**

### **3.2.2 Effect of membrane pore size**

**Fig. 5**

Fig. 5 shows the effect of membrane pore size (CM5, CM50 and CM150) on the flux curves and fouling resistances in the systems of UF and FPUF. It can be seen in Fig. 5(a) that less flux reduction occurred with higher MWCO membranes, which was likely attributed to the reason that more pollutants were retained by membranes with smaller pores. At the end of single UF, the  $J_t/J_0$  values were reduced to 0.36, 0.58 and 0.60 for CM5, CM50 and CM150, respectively. Fe(II)/PMS pretreatment significantly improved the flux of UF membranes with different MWCO, and the  $J_t/J_0$  values increased from 0.36–0.60 to 0.65–0.83. In the system of FPUF, the flux decline for CM50 was even lower than for CM150, which was likely due to the lower initial membrane flux of CM50, thus the flux variation was not so significant compared with CM150, leading to a lower flux decline. The results of fouling resistance distributions are shown in Fig. 5(b). It seemed that irreversible fouling occupied a dominant role compared with reversible fouling. During single UF, the fouling resistance significantly decreased with the increase of membrane pore size, and the average  $R_t$  values were 8.43, 1.62 and  $0.78 \times 10^{12} \text{ m}^{-1}$  for CM5, CM50 and CM150, respectively. Feed water pretreatment with Fe(II)/PMS dramatically reduced the values of  $R_t$ ,  $R_r$  and  $R_{ir}$ , regardless of membrane pore size. For membranes with MWCO of 5, 50 and 150 kDa, the reduction rates of  $R_t$  were 69%, 69% and 49%, respectively. These results indicated that Fe(II)/PMS pretreatment was very effective for improving the flux and mitigating both reversible and irreversible membrane fouling, independent of membrane pore size.

### 3.2.3 Effect of membrane surface hydrophobicity

**Fig. 6**

The effect of surface hydrophobicity on membrane fouling control by Fe(II)/PMS pretreatment was investigated, and the results are illustrated in Fig. 6. Compared to the CM150 membrane, the PES150 membrane exhibited a faster flux decline in both UF and FPUF systems. The  $J_t/J_0$  value of PES150 was much lower than that of CM150 (0.27 and 0.53 cf. 0.60 and 0.72) (Fig. 6(a)). This phenomenon was consistent with the general recognition that stronger membrane surface hydrophilicity contributed to fouling control (Xiao et al., 2011). Similar with the above results, FPUF also showed better performance in flux improvement than single UF, regardless of membrane surface hydrophobicity. As shown in Fig. 6(b), the  $R_t$ ,  $R_r$  and  $R_{ir}$  values of PES150 in single UF were significantly higher than that of CM150, indicating that hydrophobic membrane exhibited a higher fouling potential than hydrophilic membrane. As PES150 was more hydrophobic than CM150, the hydrophobic interaction between the PES150 membrane and the organic matter might be much stronger, leading to higher fouling resistance. It can be seen that both reversible and irreversible fouling were significantly mitigated by Fe(II)/PMS pretreatment. The average  $R_t$  values for PES150 and CM150 in single UF were 1.36 and  $0.78 \times 10^{12} \text{ m}^{-1}$ , respectively, and the values were correspondingly reduced to 0.48 and  $0.40 \times 10^{12} \text{ m}^{-1}$  by Fe(II)/PMS pretreatment. It seemed that the proportion of irreversible fouling for CM150 was higher than that of PES150, likely due to the structural discrepancy between ceramic and polymeric membranes. The results suggested that although membrane fouling was affected by membrane surface



hydrophobicity, the performance of Fe(II)/PMS pretreatment for membrane fouling control was insusceptible.

### 3.3 Characterization of membrane fouling

**Fig. 7**

The fluorescence EEM spectra of hydraulic irreversible foulants in different systems are shown in Fig. 7. For all the samples, peaks T1 (Ex/Em = 225/350 nm) and T2 (Ex/Em = 275/350 nm) played a dominant role in the EEM spectra, and both of the two peaks were derived from protein-like substances (Chen et al., 2003). Although humic-like substances were identified in the feed water, the corresponding peaks were not detected in the spectra (Fig. 7). Therefore, the fluorescent dissolved organic matter in the hydraulic irreversible foulants for the systems of UF, FPUF, CUF and OUF was mainly composed of protein-like substances, rather than humic-like substances. The fluorescence peak intensity followed the order of UF (T1 = 917, T2 = 658) > CUF (T1 = 821, T2 = 587) > OUF (T1 = 484, T2 = 379)  $\approx$  FPUF (T1 = 494, T2 = 350), indicating that pretreatments prior to UF membrane decreased the fluorescence intensity of irreversible organic foulants. However, the result seemed inconsistent with the hydraulic irreversible fouling resistance of different systems (Fig. 4(b)), which showed that the irreversible fouling of OUF was significantly higher than that of CUF. This phenomenon was likely attributed to the significant change of fluorescence properties by pre-ozonation, resulting in the reduction of fluorescence intensity, rather than the irreversible organic foulants.

Fig. S3 shows the SEC-UV chromatograms for hydraulic irreversible foulants.

For both UF and FPUF systems, the UV responses of biopolymers, humic acid and building blocks were apparently detected in the chromatograms. The detection of biopolymers was likely due to the accumulation of biopolymers (especially proteins) in the membrane pores. It also clearly illustrates that the overall UV response in the UF system was obviously higher than the FPUF system. This result indicated that less organic matter was retained or adsorbed in membrane pores by the application of Fe(II)/PMS process prior to UF membrane, resulting in less hydraulic irreversible fouling. All these results suggested that pretreatment prior to UF membrane plays an important role in the reduction of hydraulic irreversible foulants, and the Fe(II)/PMS process exhibited prominent performance.

It should be noted that this study was performed in a batch system. There might be some discrepancies between the obtained results in this study and continuous operation for full-scale applications. Therefore, a further systematic study on continuous operation should be conducted to evaluate the effectiveness of Fe(II)/PMS as a membrane pretreatment process for full-scale applications.

#### **4. Conclusions**

This paper has studied the performance of Fe(II)-activated PMS as a pretreatment strategy for UF membrane, as well as coagulation and ozonation for comparison. The pollutants removal efficiency and membrane fouling control were evaluated, and the following conclusions can be drawn:

(1) Fe(II)/PMS showed the best ability to remove the permeate DOC compared to conventional coagulation and ozonation, which was likely caused by the dual

functions of coagulation and oxidation in the single process; whereas the fluorescent and UV-absorbing organic components were more susceptible to ozonation than Fe(II)/PMS treatment, likely due to the stronger oxidability of ozone.

(2) Single UF showed a poor removal performance of ATZ, *p*-CNB and SMT (4.9–7.1%), and pretreatments with Fe(II)/PMS and ozonation significantly increased the efficiency by 12–76% and 50–94%, respectively. The micropollutants were mainly removed by pre-oxidation, whereas pre-coagulation exerted a minor influence.

(3) Pretreatments prior to UF attributed to the reduction of total membrane fouling (25–69%). However, pre-ozonation showed limited effect on irreversible fouling, likely due to the generation of low MW substances to accumulate within membrane pores. Fe(II)/PMS pretreatment showed the best performance for the reduction of both reversible and irreversible fouling in comparison with coagulation and ozonation.

(4) The fouling mitigation efficiency of Fe(II)/PMS pretreatment was hardly affected by the properties of employed UF membranes, such as membrane pore size and surface hydrophobicity.

(5) The hydraulic irreversible foulants mainly consisted of protein-like substances, rather than humic-like substances. Fe(II)/PMS pretreatment could significantly reduce membrane foulants.

## Acknowledgements

This research was jointly supported by the National Science Foundation for the Outstanding Youngster Fund (51522804), the National Natural Science Foundation of

508 China (51378140), HIT Environment and Ecology Innovation Special Funds  
509 (HSCJ201603) and Fundamental Research Funds for the Central Universities.

510 **Appendix A. Supplementary information**

511 Supplementary data associated with this article can be found in the online  
512 version.

## References

- Acero, J.L., Javier Benitez, F., Real, F.J., Teva, F., 2012. Coupling of adsorption, coagulation, and ultrafiltration processes for the removal of emerging contaminants in a secondary effluent. *Chem. Eng. J.* 210, 1-8.
- Anipsitakis, G.P., Dionysiou, D.D., 2003. Degradation of Organic Contaminants in Water with Sulfate Radicals Generated by the Conjunction of Peroxymonosulfate with Cobalt. *Environ. Sci. Technol.* 37(20), 4790-4797.
- Anipsitakis, G.P., Dionysiou, D.D., 2004. Radical generation by the interaction of transition metals with common oxidants. *Environ. Sci. Technol.* 38(13), 3705-3712.
- Antoniou, M.G., de la Cruz, A.A., Dionysiou, D.D., 2010. Degradation of microcystin-LR using sulfate radicals generated through photolysis, thermolysis and  $e^-$  transfer mechanisms. *Appl. Catal. B* 96(3-4), 290-298.
- Ball, R.E., Edwards, J.O., Haggett, M.L., Jones, P., 1967. A kinetic and isotopic study of the decomposition of monoperoxyphthalic acid. *J. Am. Chem. Soc.* 89(10), 2331-2333.
- Barhoumi, N., Oturan, N., Olvera-Vargas, H., Brillas, E., Gadri, A., Ammar, S., Oturan, M.A., 2016. Pyrite as a sustainable catalyst in electro-Fenton process for improving oxidation of sulfamethazine. Kinetics, mechanism and toxicity assessment. *Water Res.* 94, 52-61.
- Chen, W., Westerhoff, P., Leenheer, J.A., Booksh, K., 2003. Fluorescence excitation-emission matrix regional integration to quantify spectra for dissolved organic matter. *Environ. Sci. Technol.* 37(24), 5701-5710.

- Cheng, X., Liang, H., Ding, A., Qu, F., Shao, S., Liu, B., Wang, H., Wu, D., Li, G., 2016. Effects of pre-ozonation on the ultrafiltration of different natural organic matter (NOM) fractions: Membrane fouling mitigation, prediction and mechanism. *J. Membr. Sci.* 505, 15-25.
- Cheng, X., Liang, H., Ding, A., Tang, X., Liu, B., Zhu, X., Gan, Z., Wu, D., Li, G., 2017. Ferrous iron/peroxymonosulfate oxidation as a pretreatment for ceramic ultrafiltration membrane: Control of natural organic matter fouling and degradation of atrazine. *Water Res.* 113, 32-41.
- Gao, W., Liang, H., Ma, J., Han, M., Chen, Z.-l., Han, Z.-s., Li, G.-b., 2011. Membrane fouling control in ultrafiltration technology for drinking water production: A review. *Desalination* 272(1-3), 1-8.
- Guan, X., Dong, H., Ma, J., Jiang, L., 2009. Removal of arsenic from water: effects of competing anions on As(III) removal in  $\text{KMnO}_4$ -Fe(II) process. *Water Res.* 43(15), 3891-3899.
- Huang, H., Schwab, K., Jacangelo, J.G., 2009. Pretreatment for Low Pressure Membranes in Water Treatment: A Review. *Environ. Sci. Technol.* 43(9), 3011-3019.
- Huber, S.A., Balz, A., Abert, M., Pronk, W., 2011. Characterisation of aquatic humic and non-humic matter with size-exclusion chromatography-organic carbon detection-organic nitrogen detection (LC-OCD-OND). *Water Res.* 45(2), 879-885.
- Ji, Y., Ferronato, C., Salvador, A., Yang, X., Chovelon, J.M., 2014. Degradation of ciprofloxacin and sulfamethoxazole by ferrous-activated persulfate: implications for remediation of groundwater contaminated by antibiotics. *Sci. Total Environ.* 472,

557 800-808.

558 Ji, Y., Dong, C., Kong, D., Lu, J., 2015. New insights into atrazine degradation  
559 by cobalt catalyzed peroxymonosulfate oxidation: kinetics, reaction products and  
560 transformation mechanisms. *J. Hazard. Mater.* 285, 491-500.

561 Lee, N., Amy, G., Croue, J.P., Buisson, H., 2004. Identification and  
562 understanding of fouling in low-pressure membrane (MF/UF) filtration by natural  
563 organic matter (NOM). *Water Res.* 38(20), 4511-4523.

564 Leenheer, J.A., Croué, J.-P., 2003. Peer Reviewed: Characterizing Aquatic  
565 Dissolved Organic Matter. *Environ. Sci. Technol.* 37(1), 18A-26A.

566 Lin, C.F., Yu-Chen Lin, A., Sri Chandana, P., Tsai, C.Y., 2009. Effects of mass  
567 retention of dissolved organic matter and membrane pore size on membrane fouling  
568 and flux decline. *Water Res.* 43(2), 389-394.

569 Luo, C., Ma, J., Jiang, J., Liu, Y., Song, Y., Yang, Y., Guan, Y., Wu, D., 2015.  
570 Simulation and comparative study on the oxidation kinetics of atrazine by UV/H<sub>2</sub>O<sub>2</sub>,  
571 UV/HSO<sub>5</sub><sup>-</sup> and UV/S<sub>2</sub>O<sub>8</sub><sup>2-</sup>. *Water Res.* 80, 99-108.

572 Lutze, H.V., Bircher, S., Rapp, I., Kerlin, N., Bakkour, R., Geisler, M., von  
573 Sonntag, C., Schmidt, T.C., 2015. Degradation of chlorotriazine pesticides by sulfate  
574 radicals and the influence of organic matter. *Environ. Sci. Technol.* 49(3), 1673-1680.

575 Murphy, K.R., Butler, K.D., Spencer, R.G., Stedmon, C.A., Boehme, J.R., Aiken,  
576 G.R., 2010. Measurement of dissolved organic matter fluorescence in aquatic  
577 environments: an interlaboratory comparison. *Environ. Sci. Technol.* 44(24),  
578 9405-9412.

- 579 Neta, P., Madhavan, V., Zemel, H., Fessenden, R.W., 1977. Rate constants and  
580 mechanism of reaction of sulfate radical anion with aromatic compounds. *J. Am.*  
581 *Chem. Soc.* 99(1), 163-164.
- 582 Qu, F., Liang, H., Zhou, J., Nan, J., Shao, S., Zhang, J., Li, G., 2014.  
583 Ultrafiltration membrane fouling caused by extracellular organic matter (EOM) from  
584 *Microcystis aeruginosa*: Effects of membrane pore size and surface hydrophobicity. *J.*  
585 *Membr. Sci.* 449, 58-66.
- 586 Rastogi, A., Al-Abed, S.R., Dionysiou, D.D., 2009a. Effect of inorganic,  
587 synthetic and naturally occurring chelating agents on Fe(II) mediated advanced  
588 oxidation of chlorophenols. *Water Res.* 43(3), 684-694.
- 589 Rastogi, A., Al-Abed, S.R., Dionysiou, D.D., 2009b. Sulfate radical-based  
590 ferrous–peroxymonosulfate oxidative system for PCBs degradation in aqueous and  
591 sediment systems. *Appl. Catal. B* 85(3-4), 171-179.
- 592 Shao, S., Liang, H., Qu, F., Yu, H., Li, K., Li, G., 2014. Fluorescent natural  
593 organic matter fractions responsible for ultrafiltration membrane fouling:  
594 Identification by adsorption pretreatment coupled with parallel factor analysis of  
595 excitation–emission matrices. *J. Membr. Sci.* 464, 33-42.
- 596 Staehelin, J., Hoigne, J., 1985. Decomposition of ozone in water in the presence  
597 of organic solutes acting as promoters and inhibitors of radical chain reactions.  
598 *Environ. Sci. Technol.* 19(12), 1206-1213.
- 599 Stoquart, C., Servais, P., Bérubé, P.R., Barbeau, B., 2012. Hybrid Membrane  
600 Processes using activated carbon treatment for drinking water: A review. *J. Membr.*



- 601 Sci. 411-412, 1-12.
- 602 Tian, J.Y., Liang, H., Li, X., You, S.J., Tian, S., Li, G.B., 2008. Membrane  
603 coagulation bioreactor (MCBR) for drinking water treatment. *Water Res.* 42(14),  
604 3910-3920.
- 605 Van Geluwe, S., Braeken, L., Van der Bruggen, B., 2011. Ozone oxidation for the  
606 alleviation of membrane fouling by natural organic matter: A review. *Water Res.*  
607 45(12), 3551-3570.
- 608 Wang, H., Qu, F., Ding, A., Liang, H., Jia, R., Li, K., Bai, L., Chang, H., Li, G.,  
609 2016. Combined effects of PAC adsorption and in situ chlorination on membrane  
610 fouling in a pilot-scale coagulation and ultrafiltration process. *Chem. Eng. J.* 283,  
611 1374-1383.
- 612 Wang, Z., Chen, Z., Chang, J., Shen, J., Kang, J., Chen, Q., 2015. Fabrication of  
613 a low-cost cementitious catalytic membrane for p-chloronitrobenzene degradation  
614 using a hybrid ozonation-membrane filtration system. *Chem. Eng. J.* 262, 904-912.
- 615 Xiao, K., Wang, X., Huang, X., Waite, T.D., Wen, X., 2011. Combined effect of  
616 membrane and foulant hydrophobicity and surface charge on adsorptive fouling  
617 during microfiltration. *J. Membr. Sci.* 373(1-2), 140-151.
- 618 Xie, P., Chen, Y., Ma, J., Zhang, X., Zou, J., Wang, Z., 2016. A mini review of  
619 preoxidation to improve coagulation. *Chemosphere* 155, 550-563.
- 620 Yu, W., Graham, N.J.D., 2015. Performance of an integrated granular media –  
621 Ultrafiltration membrane process for drinking water treatment. *J. Membr. Sci.* 492,  
622 164-172.

623 Yu, W., Campos, L.C., Graham, N., 2016a. Application of pulsed UV-irradiation  
624 and pre-coagulation to control ultrafiltration membrane fouling in the treatment of  
625 micro-polluted surface water. *Water Res.* 107, 83-92.

626 Yu, W., Graham, N.J., Fowler, G.D., 2016b. Coagulation and oxidation for  
627 controlling ultrafiltration membrane fouling in drinking water treatment: Application  
628 of ozone at low dose in submerged membrane tank. *Water Res.* 95, 1-10.

629 Zhang, X., Fan, L., Roddick, F.A., 2015. Effect of feedwater pre-treatment using  
630 UV/H<sub>2</sub>O<sub>2</sub> for mitigating the fouling of a ceramic MF membrane caused by soluble  
631 algal organic matter. *J. Membr. Sci.* 493, 683-689.

632 Zou, J., Ma, J., Chen, L., Li, X., Guan, Y., Xie, P., Pan, C., 2013. Rapid  
633 acceleration of ferrous iron/peroxymonosulfate oxidation of organic pollutants by  
634 promoting Fe(III)/Fe(II) cycle with hydroxylamine. *Environ. Sci. Technol.* 47(20),  
635 11685-11691.

636 Zouboulis, A., Zamboulis, D., Szymanska, K., 2014. Hybrid membrane  
637 processes for the treatment of surface water and mitigation of membrane fouling. *Sep.*  
638 *Purif. Technol.* 137, 43-52.

639 **Table 1** Characteristics of membranes employed in this study.

Membrane	MWCO (kDa)	Contact angle (deg)	Pure water flux (L/m <sup>2</sup> h bar at 20°C)	Effective area (cm <sup>2</sup> )	Roughness (nm)
PES150	150	65.7±2.7	613.8±28	42.0	11.5
CM150	150	28.3±1.2	265.2±5.3	13.8	43.6
CM50	50	30.2±0.9	143.5±3.5	13.8	39.5
CM5	5	29.6±1.6	60.3±1.2	13.8	23.2

640

641 **Table 2** Correlation coefficient ( $R^2$ ) values of regression analyses for membrane  
642 fouling.

System	Complete blocking	Standard blocking	Intermediate blocking	Cake filtration
UF	0.952	0.998	0.961	0.970
FPUF	0.980	0.999	0.981	0.982
CUF	0.962	0.999	0.967	0.972
OUF	0.983	0.999	0.987	0.991

643

**Figure Captions**

**Fig. 1** Schematic diagram of the experimental setup.

**Fig. 2** Organic pollutants in the feed water and permeate of UF, FPUF, CUF and OUF:

(a) concentrations of DOC and  $UV_{254}$ , (b)  $F_{max}$  of fluorescent components, (c) SEC-UV chromatograms.

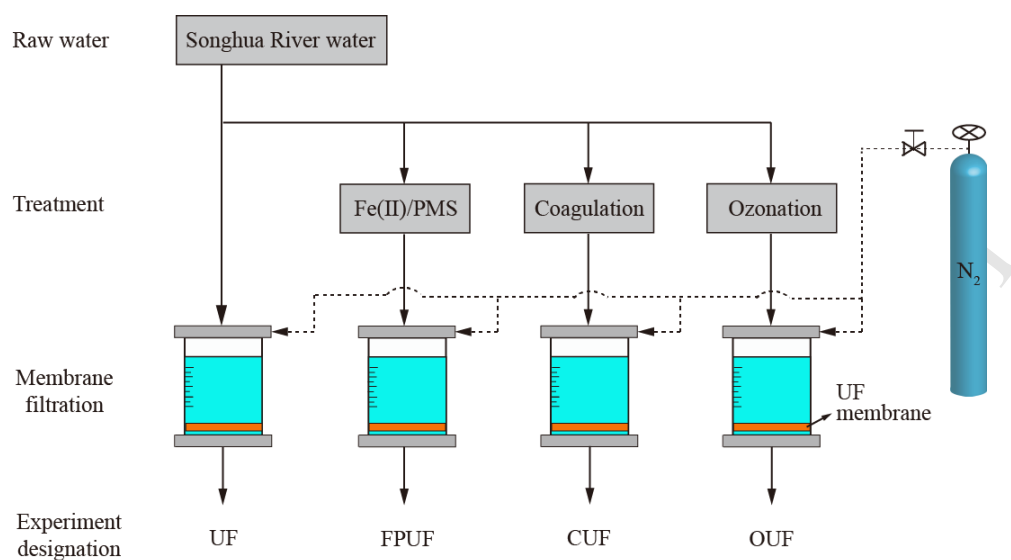
**Fig. 3** Removal efficiency of ATZ, *p*-CNB and SMT in the systems of UF, FPUF, CUF and OUF.

**Fig. 4** (a) Flux decline and (b) fouling resistance distributions in the systems of UF, FPUF, CUF and OUF.

**Fig. 5** Effect of membrane pore size on the (a) flux decline and (b) fouling resistance distributions in the systems of UF and FPUF.

**Fig. 6** Effect of membrane surface hydrophobicity on the (a) flux decline and (b) fouling resistance distributions in the systems of UF and FPUF.

**Fig. 7** Fluorescence EEM spectra of hydraulic irreversible organic foulants in the systems of UF (a), FPUF (b), CUF (c) and OUF (d).

**Fig. 1** Schematic diagram of the experimental setup.

**Fig. 2** Organic pollutants in the feed water and permeate of UF, FPUF, CUF and OUF:

(a) concentrations of DOC and UV<sub>254</sub>, (b)  $F_{max}$  of fluorescent components, (c) SEC-UV chromatograms (Error bars represent standard deviations; n=3).

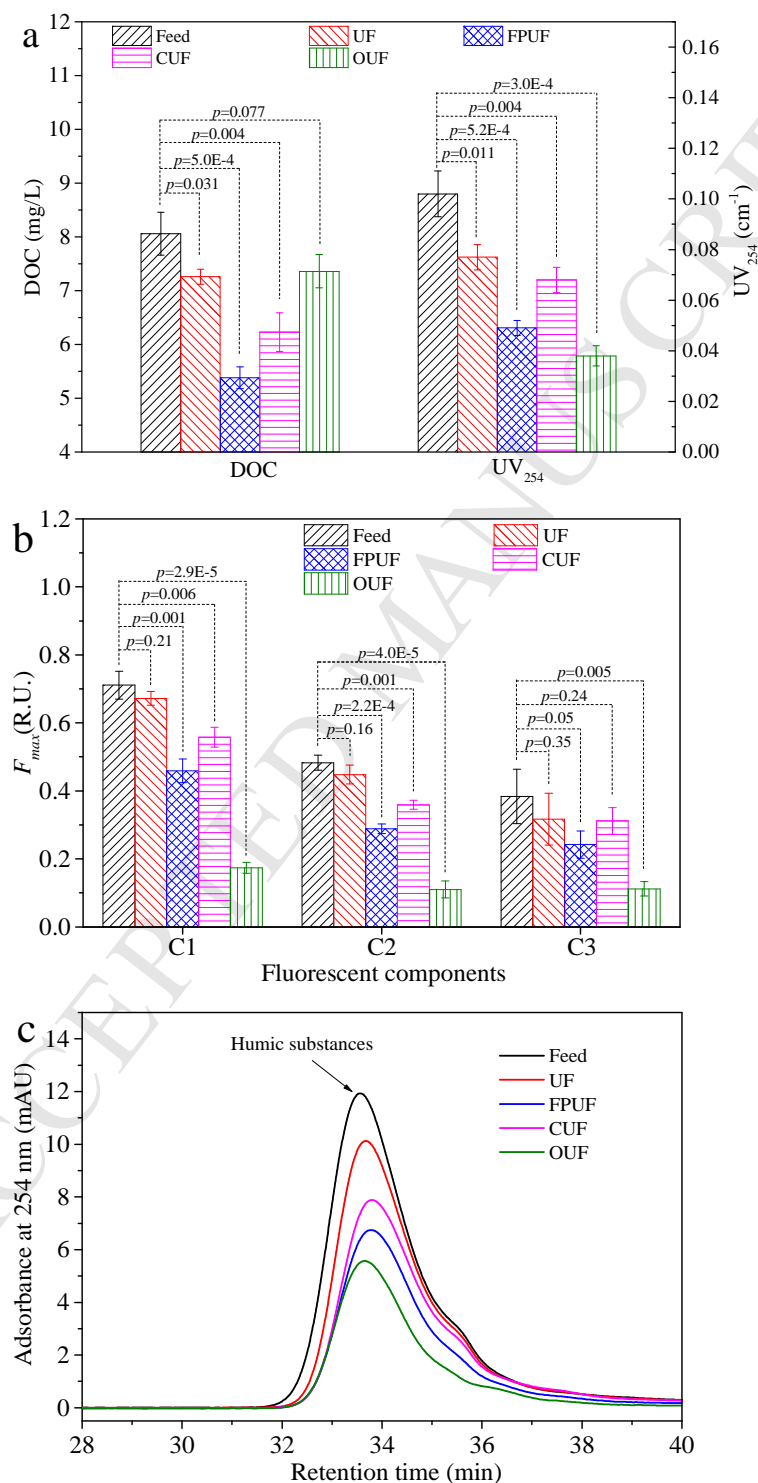


**Fig. 3** Removal efficiency of ATZ (216  $\mu\text{g/L}$ ), *p*-CNB (158  $\mu\text{g/L}$ ) and SMT (278  $\mu\text{g/L}$ ) in the systems of UF, FPUF, CUF and OUF. The employed doses of Fe(II)/PMS, Fe(III) and ozone were 50  $\mu\text{mol/L}$ , respectively (Error bars represent standard deviations;  $n=3$ ).

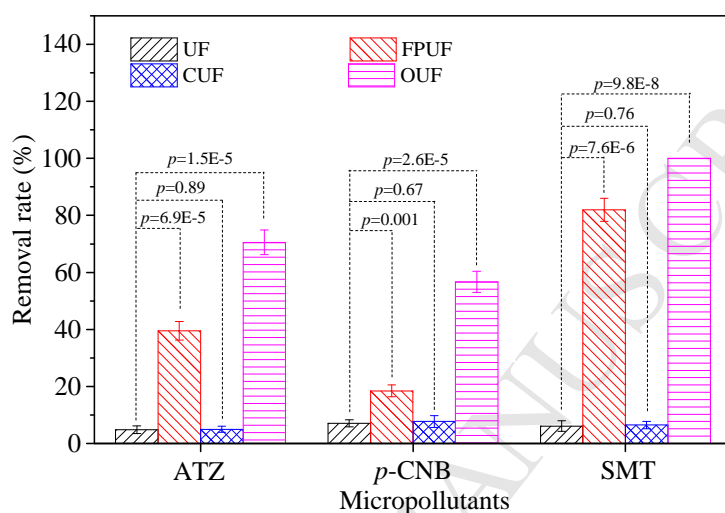


**Fig. 4** (a) Flux decline and (b) fouling resistance distributions in the systems of UF, FPUF, CUF and OUF with CM 50.

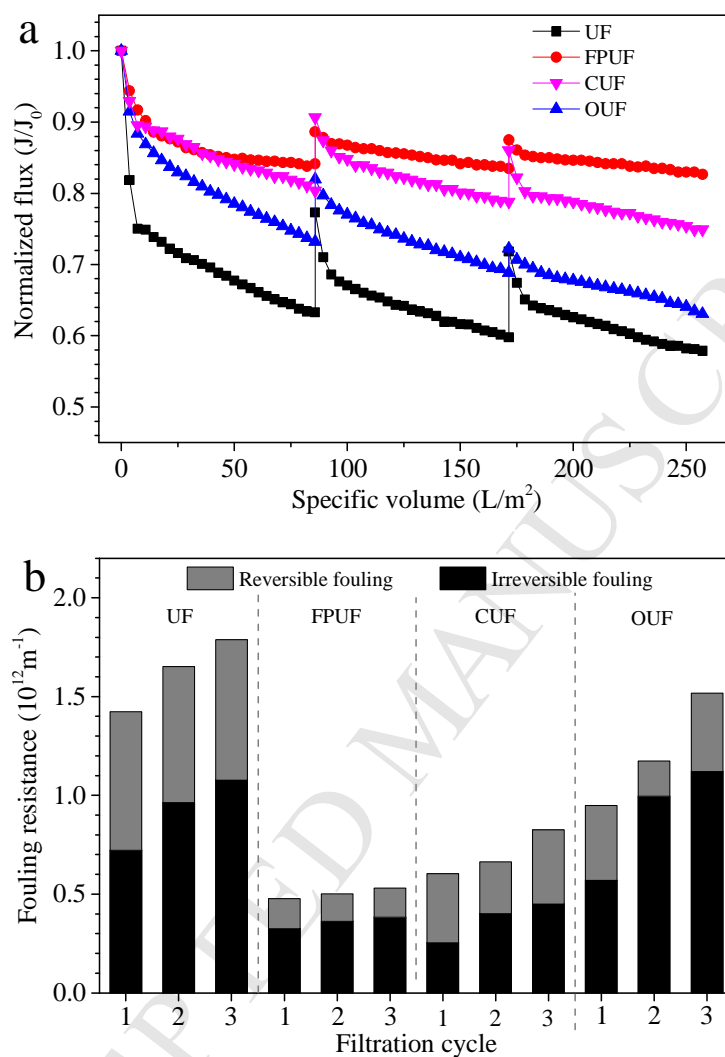




**Fig. 5** Effect of membrane pore size on the (a) flux decline and (b) fouling resistance

distributions in the systems of UF and FPUF.

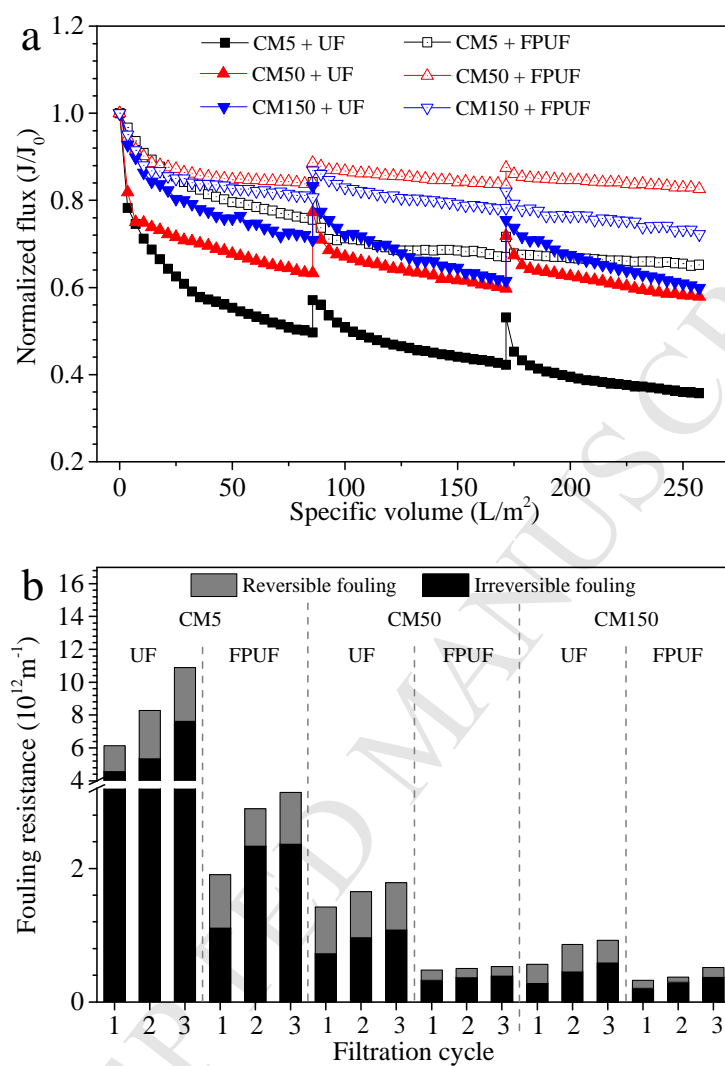


**Fig. 6** Effect of membrane surface hydrophobicity on the (a) flux decline and (b) fouling resistance distributions in the systems of UF and FPUF.

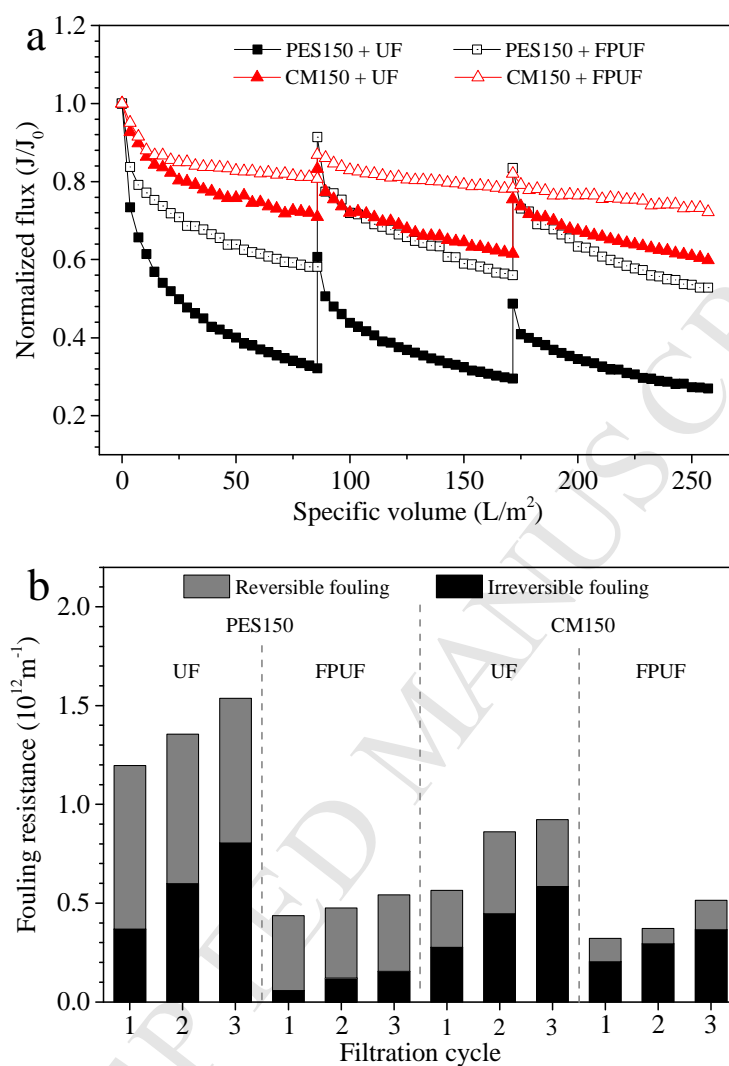
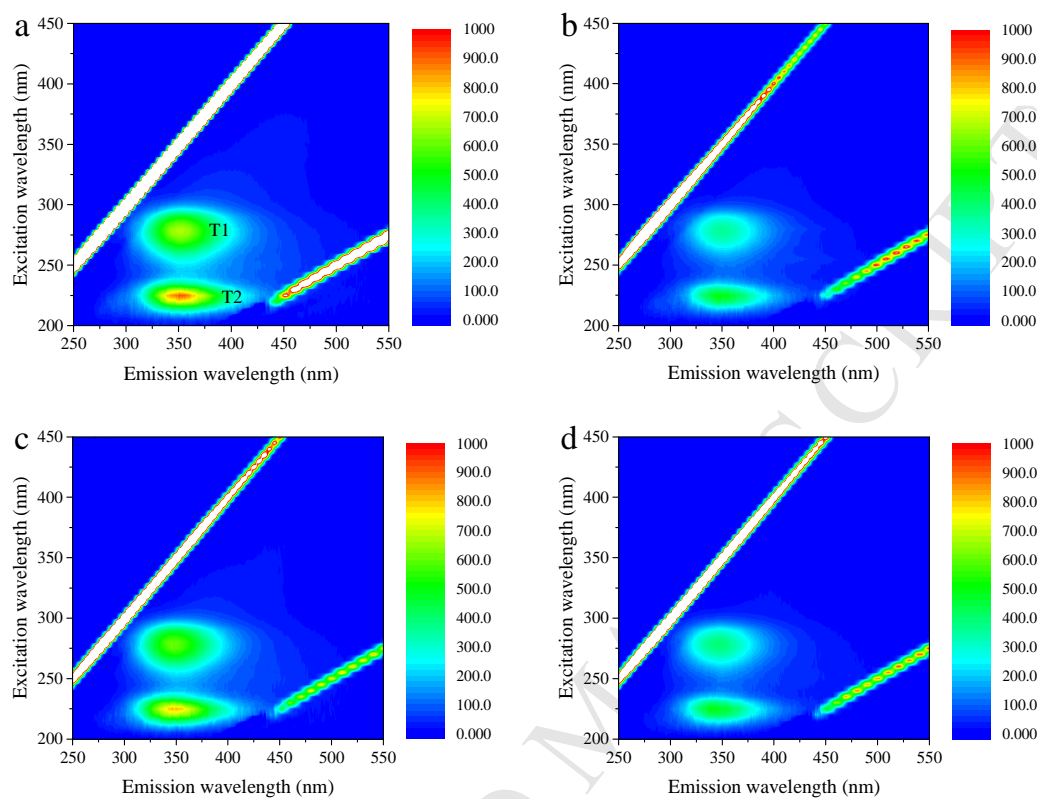


**Fig. 7** Fluorescence EEM spectra of hydraulic irreversible organic foulants in the systems of UF (a), FPUF (b), CUF (c) and OUF (d).



**Highlights**

Fe(II)/PMS was applied prior to UF membrane for treating natural surface water.

The interaction between Fe(II) and PMS promoted generation of Fe(III) and  $\text{SO}_4^{\bullet-}$ .

Fe(II)/PMS significantly improved the removal efficiency of micropollutants for UF.

Fe(II)/PMS reduced membrane fouling more efficiently than coagulation and ozonation.